The Twentieth International Symposium on Artificial Life and Robotics 2015 (AROB 20th 2015),
B-Con Plaza, Beppu, Japan, January 21-23, 2015

Development of a master controller for a dual-arm underwater robot

Radzi Bin Ambar and Shinichi Sagara
Department of Mechanical and Control Engineering,
Kyushu Institute of Technology,
Tobata, Kitakyushu 804-8550, Japan
E-mail: sagara@cntl.kyutech.ac.jp

Abstract: Master-slave system is a vital technique for controlling robot motions, especially in underwater robotics applications. This paper describes the development of a novel master controller for an experimental dual-arm underwater robot. By using the proposed master controller, a human operator is able to control an underwater robot movement in 3-dimensional space. The master controller also includes two units of 3-link manipulator controller. Moreover, each end-tips of the manipulator controller are attached with a joystick, one for controlling robot position, while the other controls robot attitude. The uniqueness of the proposed master controller is that a human operator is able to control the motion of robot base and two units of 3-link slave manipulator simultaneously. In this work, the hardware design of the proposed master controller and the structure of master-slave system are presented. The usefulness of the proposed master controller is verified through experiments on controlling an actual dual-arm underwater robot.

Keywords: Underwater Robot, Manipulator, UVMS, Control

1 Introduction

Underwater robotic technologies allow humans to execute intervention tasks in an efficient and safe way by reducing the risks of underwater operations. Intervention capabilities are necessary to execute tasks such as valve manipulation using robotic arms in oil and gas related operations; conducting science experiments or collection of rocks and marine organisms; and maybe can be deployed for deep-sea search and rescue operation. Motivated by these, our research activities are related to the development of an Underwater Vehicle-Manipulator Systems (UVMS). UVMS is an unmanned underwater vehicle equipped with one or more robotic arms for intervention task.

Researchers of UVMS technology are developing robots that can operate autonomously without any direct human intervention. Many researchers are focusing on autonomous control of underwater robot [1–4]. We have also proposed digital Resolved Acceleration Control (RAC) methods for single-arm and dual-arm UVMS [5, 6]. However, human operators are necessary for operating robotic arms because fully autonomous robotic arm manipulation technologies are still far from being perfected. Master-slave system is a common technique for controlling underwater robots. In master-slave system, a master controller is used to control the position and attitude of a robot slave in 3-dimensional space from a distance. In the field of underwater robotics, especially related to semi-autonomous underwater robots, there are not many research literatures discussing the designs and significant impact of master-slave system. In some research studies, game controllers and off-the-shelf manipulator controllers have been used as master controllers [7–9]. Moreover, many studies are focusing on developing interface devices for single-arm manipulator applications [7, 9–12]. Hence, development of a novel master controller that can control vehicle and multiple robotic arms movement simultaneously is necessary for efficient underwater intervention tasks.

In this work, we have developed a master controller for an experimental 3-link dual-arm underwater robot. By using the proposed master controller, a human operator is able to control an underwater robot movement in 3-dimensional space via master-slave system. The master controller also includes two units of 3-links manipulator master controller. Moreover, each end-tips of the master controller is attached with a joystick, one for controlling robot position, while the other controls robot attitude. The uniqueness of the proposed master controller is that the operator is able to control the motion of robot base and two units of 3-link slave manipulator simultaneously. Additionally, the control system of the robot base is based on digital Resolved Acceleration Control (RAC) method introduced in [6]. In this work, the hardware design of the proposed master controller are presented. The usefulness of the proposed master controller is verified through experiments on controlling a dual-arm underwater robot.

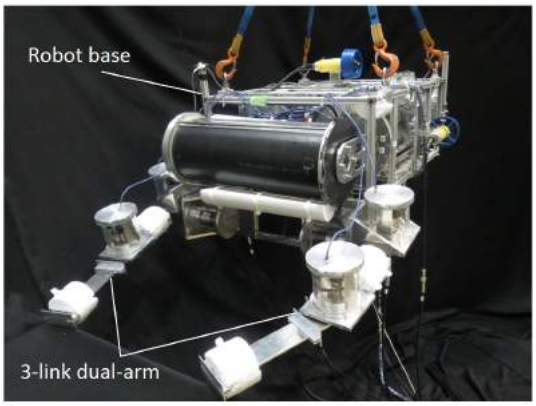

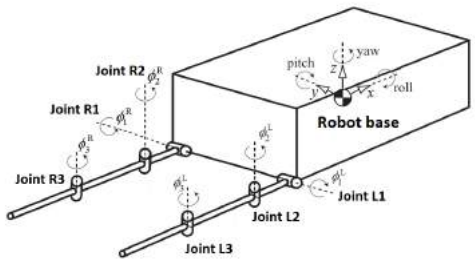

Fig. 1 3-link dual-arm underwater robot

The paper consists of three sections. In section 2, this paper describes the master-slave system of an underwater robot including the hardware design of the proposed master controller. Then, experiment method and results of the experiment are presented in section 3. Finally, conclusion is described in Section 4.

2 Master-Slave System

2.1 UVMS

Fig. 1 shows the underwater robot that is used in this work. Table 1 shows the physical parameters of the robot. The robot is consisting of a robot base (vehicle) and 2 units of 3-link manipulator. The robot is capable to move in three-dimensional space using six single propeller thrusters.

The control system for the robot base is based on RAC method proposed in [6]. The RAC method is consisting of the following equations of motion of the robot, desired acceleration $\boldsymbol{\alpha}_d(k)$ and desired velocity $\boldsymbol{\nu}_d(k)$ for robot base and both manipulator's end-tips are defined as follows:

$$\boldsymbol{u} = \boldsymbol{M}(\boldsymbol{q})\boldsymbol{\alpha}_d + \boldsymbol{N}(\boldsymbol{q},\ \boldsymbol{\zeta})\boldsymbol{\zeta} + \boldsymbol{f} \tag{1}$$

$$\boldsymbol{\alpha}_d(k) = \frac{1}{T}\boldsymbol{W}(k)^{\sharp}\{\boldsymbol{\nu}_d(k+1) - \boldsymbol{\nu}_d(k) + \boldsymbol{\Lambda}\boldsymbol{e}_{\nu}(k) + T\boldsymbol{f}(k)\} \tag{2}$$

$$\boldsymbol{\nu}_d(k) = \frac{\boldsymbol{S}_{0e}}{T}\{\boldsymbol{x}_d(k) - \boldsymbol{x}_d(k-1) + \boldsymbol{\Gamma}\boldsymbol{e}_x(k-1)\} \tag{3}$$

Table 1 Physical parameters of underwater robot

	Base	Link 1	Link 2	Link 3
Mass [kg]	104.52	5.90	2.86	1.40
Volume [$\times 10^{-3}$ m^3]	106.21	2.92	9.4	10.0
Moment of inertia (x axis) [kgm^2]	2.4	7.933 $\times 10^{-3}$	3.575 $\times 10^{-3}$	1.75 $\times 10^{-3}$
Moment of inertia (y axis) [kgm^2]	2.4	7.933 $\times 10^{-3}$	23.24 $\times 10^{-3}$	13.97 $\times 10^{-3}$
Moment of inertia (z axis) [kgm^2]	2.4	7.368 $\times 10^{-3}$	23.24 $\times 10^{-3}$	13.97 $\times 10^{-3}$
Link length (x axis) [m]	0.870	0.093	0.305	0.335
Link length (y axis) [m]	0.640	-	-	-
Link length (z axis) [m]	0.335	-	-	-
Link diameter[m]	-	0.10	0.10	0.10
Added mass(x) [kg]	73.19	0.730	0.333	0.333
Added mass(y) [kg]	30.57	0.730	2.356	2.631
Added mass(z) [kg]	99.54	0.333	2.356	2.631
Added moment of inertia (x) [kgm^2]	0.64	0.077 $\times 10^{-3}$	2.454 $\times 10^{-3}$	2.454 $\times 10^{-3}$
Added moment of inertia (y) [kgm^2]	1.28	0.077 $\times 10^{-3}$	27 $\times 10^{-3}$	46.88 $\times 10^{-3}$
Added moment of inertia (z) [kgm^2]	0.64	2.4 $\times 10^{-3}$	27 $\times 10^{-3}$	46.88 $\times 10^{-3}$
Drag coefficient(x)	1.2	1.0	1.0	1.0
Drag coefficient(y)	1.2	1.0	1.0	1.0
Drag coefficient(z)	1.2	1.0	1.0	1.0

where for Eq. (1) $\boldsymbol{q} = [\boldsymbol{x}_0^T,\ \boldsymbol{\phi}^T]^T$ and $\boldsymbol{\zeta} = [\dot{\boldsymbol{v}}_0^T,\ \dot{\boldsymbol{\phi}}^T]^T$, $\boldsymbol{x}_0$ is the position and attitude vector of robot base, $\boldsymbol{\phi}$ is the relative joint angle vector, $\boldsymbol{v}_0$ is the linear and angular vector of robot base, $\boldsymbol{M}$ is the inertia matrix including the added mass and inertia, $\boldsymbol{N}(\boldsymbol{q},\boldsymbol{\zeta})\boldsymbol{\zeta}$ is the vector of Coliolis and centrifugal forces, $\boldsymbol{f}$ is the vector consisting of the drag, gravitational and buoyant forces and moments, $\boldsymbol{u} = [\boldsymbol{f}_0^T,\ \boldsymbol{\tau}_0^T, \boldsymbol{\tau}_m^T]^T$, $\boldsymbol{f}_0$ and $\boldsymbol{\tau}_0$ are the force and torque vectors of vehicle, $\boldsymbol{\tau}_m$ is the joint torque vector of manipulator. For Eqs. (2) and (3) $\boldsymbol{e}_{\nu}(k) = \boldsymbol{\nu}_d(k) - \boldsymbol{\nu}(k)$ and $\boldsymbol{e}_x(k) = \boldsymbol{x}_d(k) - \boldsymbol{x}(k)$. Here, $\boldsymbol{\nu} = \left[\boldsymbol{\nu}_0^T,\ \boldsymbol{\nu}_e^T\right]^T$, $\boldsymbol{\nu}_e$ is the linear and angular vector of manipulator end-tips, $\boldsymbol{x}_e$ is the position and attitude vector of manipulator end-tips. $\boldsymbol{x}_d$ is the desired value of $\boldsymbol{x} = [\boldsymbol{x}_0^T,\ \boldsymbol{x}_e^T]^T$, $\boldsymbol{\Lambda} = \mathrm{diag}\{\lambda_i\}$ and $\boldsymbol{\Gamma} = \mathrm{diag}\{\gamma_i\}$ (i =1, $\cdots$, 12) are the velocity and the position feedback gain matrices. Furthermore, T is data sampling period and transformation matrix $\boldsymbol{S}_{0e} = \mathrm{blockdiag}\{\boldsymbol{E}_3, \boldsymbol{S}_{\psi 0}, \boldsymbol{E}_3, \boldsymbol{S}_{\psi e_{\mathrm{R}}}, \boldsymbol{E}_3, \boldsymbol{S}_{\psi e_{\mathrm{L}}}\}$, where

$$\boldsymbol{S}_{\boldsymbol{\psi}_{\dagger}} = \begin{bmatrix} \cos\psi_{p_{\dagger}}\cos\psi_{p_{\dagger}} & -\sin\psi_{y_{\dagger}} & 0 \\ \cos\psi_{p_{\dagger}}\sin\psi_{p_{\dagger}} & \cos\psi_{y_{\dagger}} & 0 \\ \sin\psi_{p_{\dagger}} & 0 & 1 \end{bmatrix}.$$

($\dagger$ = 0(=robot base), e_{R}(=right arm end-tip), e_{L}(=left arm end-tip)), $\boldsymbol{\psi}_{\dagger}$ is attitude vector of robot base and manipulator's end-tips, $\boldsymbol{E}_3$ is 3×3

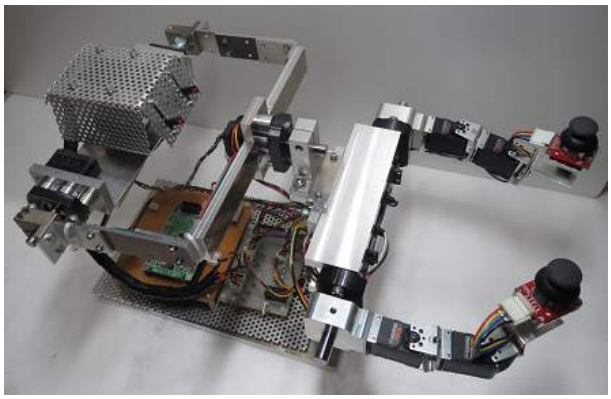

Fig. 2 Master Controller

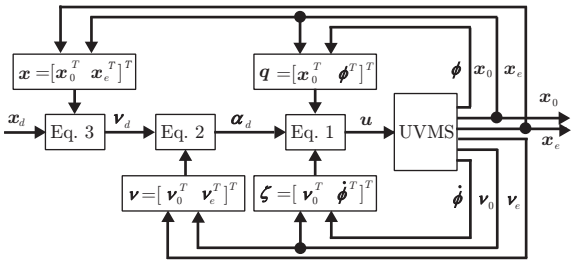

Fig. 3 RAC method block diagram.

unit matrix, $\boldsymbol{W}^{\sharp}$ is the pseudoinverse of $\boldsymbol{W}$, i.e. $\boldsymbol{W}^{\sharp} = \boldsymbol{W}^{T}(\boldsymbol{W}\boldsymbol{W}^{T})^{-1}$, where

$$\boldsymbol{W} = \begin{bmatrix} \boldsymbol{C} + \boldsymbol{E_6} & \boldsymbol{D} \\ \boldsymbol{A} & \boldsymbol{B} \end{bmatrix}.$$

Here, $\boldsymbol{A}$ and $\boldsymbol{B}$ are matrices consist of position and attitude of robot base and manipulator's joint angles, respectively. $\boldsymbol{C}$ is matrix for mass and $\boldsymbol{D}$ is matrix for inertia momentum. Both $\boldsymbol{C}$ and $\boldsymbol{D}$ matrices are included with hydrodynamic added mass and added inertia momentum which we assumed to be constant. Detail explanations regarding the symbols in the matrices can be found in [6]. Fig. 3 shows the block diagram of the RAC method.

2.2 Master controller

Fig. 2 shows the novel master controller developed in this work, consisting of a robot base main master controller, 2 units of manipulator master controller and 2 units of robot base secondary master controller.

Fig. 4(a) shows the robot base main master controller. The robot base controller enables the user to control the motion of a slave robot in 3-dimensional space (3-DOF position and 3-DOF attitude) using only one hand. First, the translational motion of a robot (x, y and z axes) can be controlled using three slide-type potentiometers installed on a box-shaped controller of the robot base controller as shown in Fig. 4(b). The translational speed of the robot is

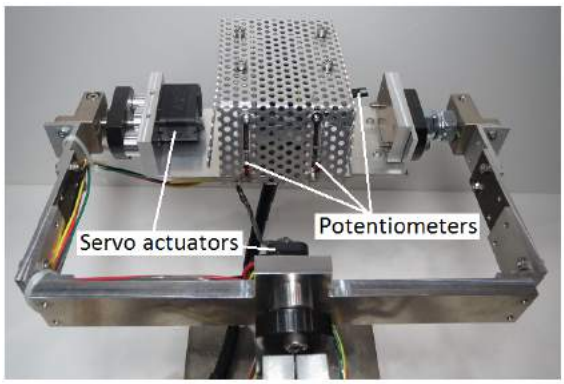

(a) Robot base controller

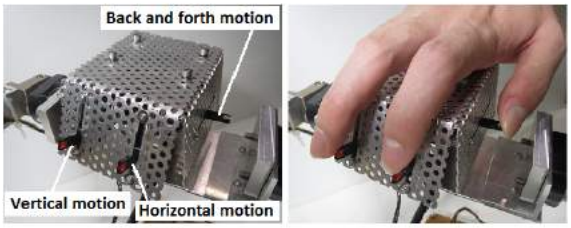

(b) Translational motions

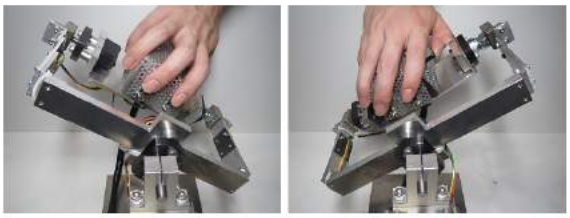

(c) Roll motion

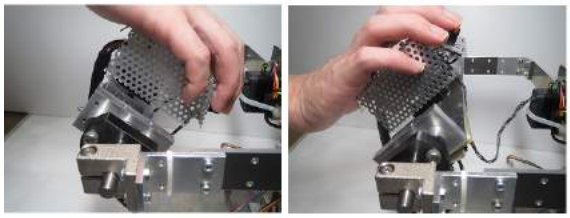

(d) Pitch motion

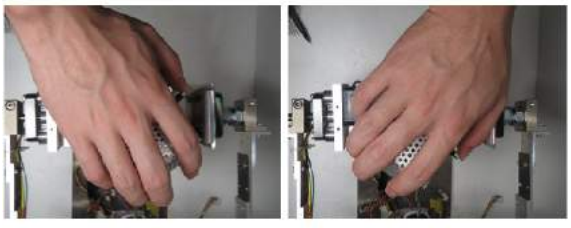

(e) Yaw motion

Fig. 4 Robot base main master controller

proportional to the changes of electrical potential (voltage) from the potentiometers. Thus, the translational speed of the robot base can be controlled by adjusting the slide potentiometer levers. The robot base controller is also consists of three servo actuators as shown in Fig. 4(a). The third servo is installed inside the box-shaped controller. The servos

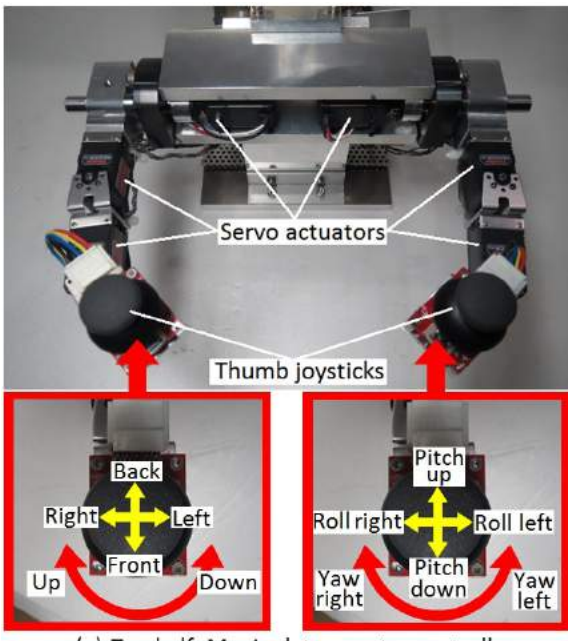

(a) Top half: Manipulator master controller.
Below half: Robot bas secondary master controller

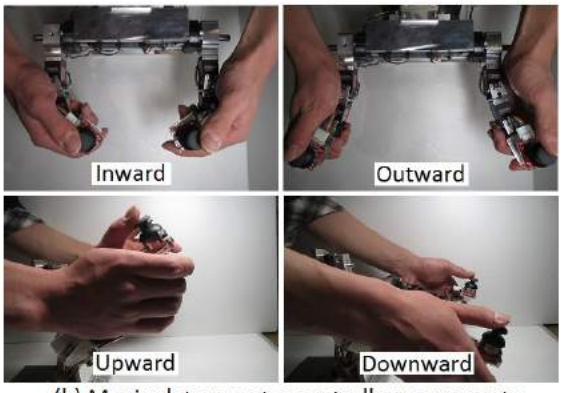

(b) Manipulator master controller movements

Fig. 5: Manipulator master controller and robot base secondary master controller

were arranged so that the axes is perpendicular to the center of the box-shaped controller. These servo actuators enable the control of rotational motion of the robot base (roll, pitch and yaw angles). Fig. 4(c) to (e) show the rotational motion when using the robot base main master controller.

Top half of Fig. 5(a) shows the 3-link dual-arm manipulator master controller. Each of the joints of the manipulator is consists of an RC servo actuator. These servo actuators are used to provide the desired joint angles for the manipulators of the slave robot including keeping any desired postures of the slave robot manipulators. Fig. 5(b) shows the manipulator master controller movements. Furthermore, at the end of each end-tips of the manipulator master controller is a robot base secondary master controller consists of a thumb joystick and a shaft potentiometer. These secondary controllers have similar functions as the robot base main controller which are to

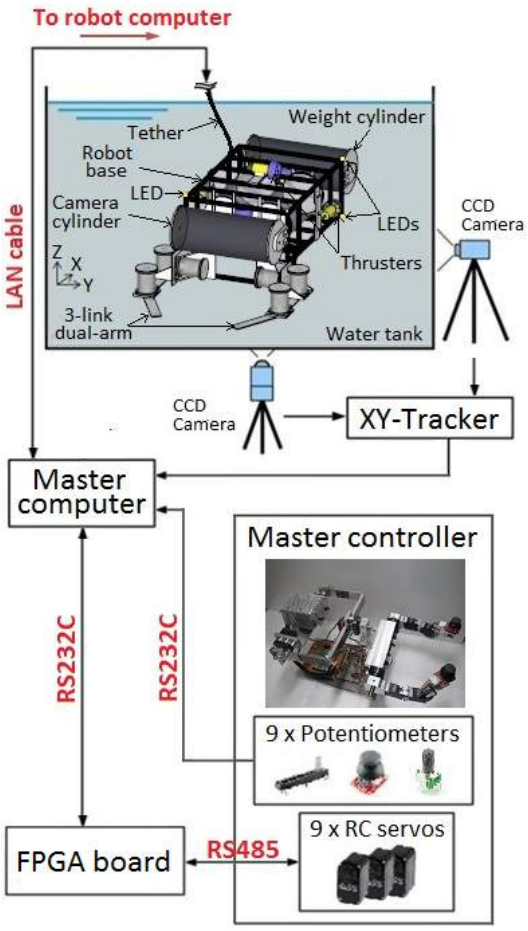

Fig. 6 Structure of the master-slave system

control robot base position and attitude. Below half of Fig. 5(a) shows the functionality of the controllers.

Fig. 6 shows the structure of the master-slave system. A total of 9 units of servo actuators and 9 units of potentiometers are used in the proposed master controller. All potentiometers data are sent to A/D converter of a surface master computer. On the other hand, all servo actuators are connected to the master computer via an FPGA board. FPGA board is used to convert RS485 data signals into RS232 signals and vice versa.

3 Experiments

The experiment for verifying the effectiveness of the developed master controller on controlling an actual 3-link dual-arm underwater robot was conducted based on the experimental setup shown in Fig. 6. The experiment was carried out in a water tank. The tank specifications are 3[m] width, 2[m] length and 2[m] depth. The position and attitude of the robot can be calculated by monitoring the movement of three LEDs light sources via CCD cameras. The data from CCD cameras were converted to position data using an X-Y video tracker. The data sampling

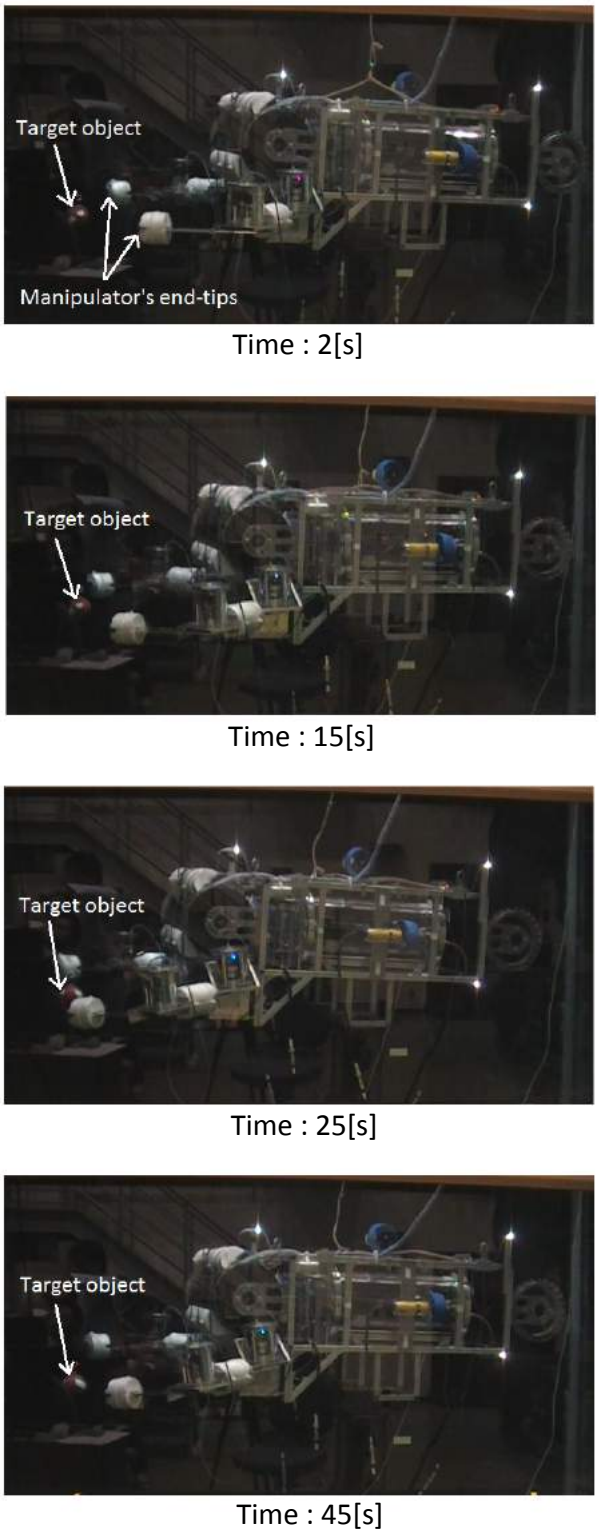

Fig. 7 UVMS motion during experiment.

period was $T = 1/20$[s].

In the experiment, an operator was asked to perform a simple task of moving both end-tips of the slave manipulator to a target object using the master controller. The operator was asked to use (a) the robot base secondary master controller to move the robot base and, (b) manipulator master controller to move the slave manipulator. Fig. 7 shows image sequences taken from video footage during the experiment. The master-slave operations started 2[s] from the start of the experiment. These images demonstrate that the robot was controlled to move towards the target object. After 25[s], both end-tips of the manipulator were controlled to be in the vicinity of the target object successfully. These can be further verified by observing the desired and actual manipulator joint angles data as shown in Fig. 8. Fig. 8(b) shows that the slave manipulator followed the desired joint angles of the manipulator master controller shown in Fig. 8(a). Furthermore, Fig. 9 show the time histories of the robot position and attitude during the experiment. The results demonstrate that the actual robot position and attitude correspond to the desired position and attitude. However, the robot demonstrate large vibration during experiment due to the effect of the long data sampling period. Moreover, during the experiment, the operator only controlled the translational motion of the robot. Unfortunately, in Fig. 9(c), instead of producing 0[deg] results during the experiment, the desired rotational motions (roll, pitch and yaw angles) from the potentiometers produced inaccurate readings due to the inaccurate mapping of the potentiometer values with the required attitude angles. For future work, improvement on this area will be implemented. Nevertheless, the preliminary experiment demonstrate that the operator was able to control the robot base and both end-tips of the manipulator simultaneously using the robot base secondary master controller and manipulator master controller.

4 Conclusion

In this work, we have proposed a master controller for a 3-link dual-arm underwater robot. By using the proposed master controller, an operator is able to control an underwater robot movement in 3-dimensional space. The master controller also includes two units of 3-links replica master arm. The uniqueness of the proposed master controller is that a human operator is able to control two units of 3-link manipulator and also controls the motion of underwater robot simultaneously. The usefulness of the proposed master controller was verified through experiments on controlling an actual 3-link dual-arm underwater robot.

References

[1] H. Maheshi *et al.*, "A Coordinated Control of an Underwater Vehicle and Robotic Manipulator", *J. Robotic Systems*, Vol. 8, No. 3, pp. 339 – 370, 1991.

[2] T. W. McLain *et al.*, "Experiments in the Coordinated Control of an Underwater Arm/Vehicle System", *Autonomous Robots 3*, Kluwer Academic Publishers, pp. 213 – 232, 1996.

[3] G. Antonelli *et al.*, "Tracking Control for Underwater Vehicle-Manipulator Systems with Velocity Estimation", *IEEE J. Oceanic Eng.*, Vol. 25, No. 3, pp. 399 – 413, 2000.

[4] N. Sarkar and T. K. Podder, "Coordinated Motion Planning and Control of Autonomous Underwater Vehicle-Manipulator Systems Subject to Drag Optimization", *IEEE J. Oceanic Eng.*, Vol. 26, No. 2, pp. 228 – 239, 2001.

[5] S. Sagara *et al.*,"Digital RAC for Underwater Vehicle-Manipulator Systems Considering Singular Configuration", *J. Artificial Life and Robotics*, Vol. 10, No. 2, pp. 106 – 111, 2006.

[6] S. Sagara and R. Bin Ambar,"Digital Resolved Acceleration Control of Underwater Robot with multiple manipulators", *Proc. of 2014 Int. Conf. on Advanced Mechatronic Systems (ICAMechS)*, pp. 232-237, 2014.

[7] S.-U. Lee *et al.*,"Development of a Tele-operated Underwater Robotic System for maintaining a light-water type power reactor", *Proc. of Int. Joint Conf. SICE-ICASE*, pp. 3017-3021, 2006.

[8] B. H. Jun *et al.*, "Workspace control system of underwater tele-operated manipulators on ROVs", *Proc. of OCEANS 2009-EUROPE*, pp. 1-6, 2009.

[9] F. Takemura and R. T. Shiroku, "Development of the actuator concentration type removable underwater manipulator", *Proc. of 11th Int. Conf. on Control Automation Robotics and Vision (ICARCV)*, pp. 2124-2128, 2010.

[10] S. Soylu *et al.*, "Comprehensive underwater vehicle-manipulator system teleoperation", *Proc. of OCEANS 2010*, pp. 1-8, 2010.

[11] J. J. Yao *et al.*,"Development of a 7-function hydraulic underwater manipulator system" *Proc. of 2009 IEEE Int. Conf. on Mechatronics and Automation*, pp. 1202-1206, 2009.

[12] K. Kawano, T. Shimozawa, and S. Sagara, "A Master-Slave Control System for a Semi-Autonomous Underwater Vehicle-Manipulator System", *Artificial Life and Robotics*, Vol.16, pp. 465-468, 2012.

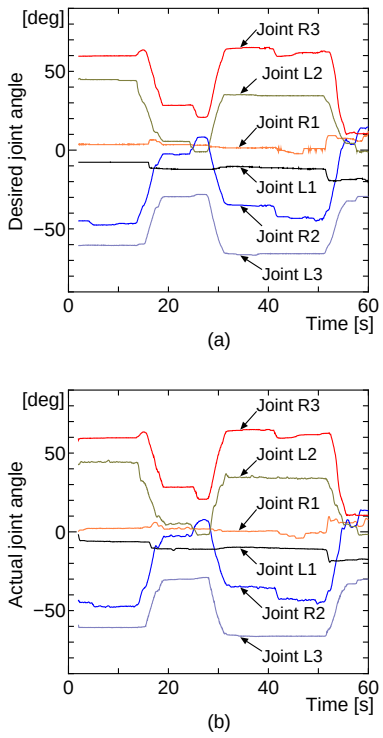

Fig. 8 Time history of manipulator's joint angles

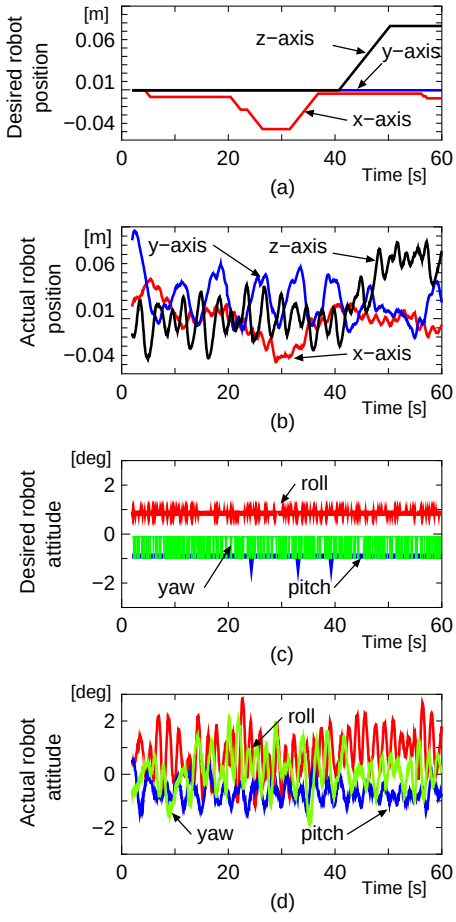

Fig. 9: Time history of position and attitude for robot base